Case Studies in Construction Materials 22 (2025) e04792

Contents lists available at ScienceDirect

Case Studies in Construction Materials

journal homepage: www.elsevier.com/locate/cscm

Statistical analysis of an in-vehicle image-based data collection method for assessing airport pavement condition

Ianca Feitosa [a,b,*], Bertha Santos [a,b,c], Jorge Gama [d], Pedro G. Almeida [a,b]

[a] University of Beira Interior, Department of Civil Engineering and Architecture, Covilhã 6200-358, Portugal
[b] GEOBIOTEC, Department of Civil Engineering and Architecture, University of Beira Interior, Covilhã, Portugal
[c] CERIS, Instituto Superior Técnico, University of Lisbon, Lisbon 1049-001, Portugal
[d] Centre of Mathematics and Applications, University of Beira Interior, Covilhã 6201-001, Portugal

ARTICLE INFO

Keywords:
Airport pavement inspection
Pavement distress
Data collection
Image processing
Statistical methods
nparLD test
Spearman's correlation

ABSTRACT

This study presents a comprehensive comparative statistical analysis to validate a novel in-vehicle image-based method for collecting pavement condition data in airport environments. It highlights the method's potential to address key challenges faced by airport pavement managers, such as the need for continuous maintenance and the demand for fast, effective, and reliable inspection procedures. The in-vehicle system integrates laser scanning systems, image capture, and georeferencing devices to collect pavement distress data, and its accuracy and reliability are evaluated statistically. The primary objective is to validate and enhance this novel inspection approach, which shows strong potential as an effective alternative for comprehensive pavement evaluation, enabling continuous, rapid monitoring and the analysis of trends. Validation was performed by means of a detailed statistical comparison of pavement distress density on the main runway of Amílcar Cabral International Airport, Sal Island, Cape Verde, based on data collected using the proposed in-vehicle and the traditional on-foot inspection methods. Non-parametric repeated measures analysis (nparLD) showed statistically similar results between methods for 9 of 12 distress type-severity combinations (4 types × 3 levels), especially for medium and high severity cases, and that pavement section and method-section factors were significant in 10 and 9 of 12 cases, respectively, indicating spatial variability. Kruskal-Wallis tests were applied to each method separately. Significant section-based differences were found in 11 of 12 cases for the traditional method and in 2 of 12 cases for the in-vehicle image-based method, indicating greater sensitivity of the on-foot inspection to spatial variation in distress distribution. These findings support the statistical validation of the proposed method for practical application in airport pavement management. Furthermore, the comprehensive analysis, which included correlation and autocorrelation studies, revealed a bias in severity level assignment during traditional on-foot inspections. The findings highlight time-efficiency gains with the image-based method and suggest improvements, such as enhancing image quality and providing inspector training to increase the accuracy of severity level classification. These results offer valuable insights for airport pavement managers, contributing to improved safety, operational efficiency, and resilience in the face of growing air traffic demands.

* Corresponding author at: University of Beira Interior, Department of Civil Engineering and Architecture, Covilhã 6200-358, Portugal.
E-mail address: ianca.feitosa@ubi.pt (I. Feitosa).

https://doi.org/10.1016/j.cscm.2025.e04792
Received 12 March 2025; Received in revised form 1 May 2025; Accepted 14 May 2025
Available online 15 May 2025

1. Introduction

As key pillars of the global transportation system, airports play an essential role in facilitating international tourism, supporting global trade, and driving economic development. As vital connectivity hubs, they enable the rapid movement of people and goods. Moreover, airports contribute significantly to job creation, technological innovation, and national economic performance, reinforcing their strategic importance for many countries [1].

With the substantial rise in air travel demand, airports face increasing challenges, such as the need for effective pavement management, infrastructure modernization, and the adoption of sustainable practices to reduce environmental impacts. According to the International Air Transport Association (IATA), global air traffic is expected to double by 2037 [2]. In March 2023 alone, total air traffic increased by 52.4 % compared to March 2022, with domestic and international traffic growing by 34.1 % and 68.9 %, respectively [3]. This trend places considerable pressure on airport infrastructure and underscores the critical importance of maintaining pavement conditions to ensure safety and operational efficiency.

The rising number of aircraft movements accelerates runway deterioration, making frequent maintenance essential to preserve surface quality. If not adequately managed, pavement distress can lead to surface irregularities that compromise flight safety. Deformations, cracks and debris pose significant risks during landing and takeoff, potentially causing incidents such as skidding or trajectory deviations [4–9]. To address these concerns, airports are implementing new preventive strategies, including routine inspections, preventive repairs, and timely replacement of deteriorated areas. In addition, upgrades may be necessary to accommodate the operational demands of larger and heavier aircraft [3,4,8–11]. The intensive use of runways, combined with projected traffic growth, highlights the urgent need for effective maintenance strategies based on fast, cost-efficient and reliable data collection methods [2–6,12–15].

In this context, Airport Pavement Management Systems (APMS) are fundamental tools for preserving runway performance and longevity. These systems support strategic long-term planning to address evolving aviation needs, ensure compliance with regulatory standards, and optimize maintenance and operational activities [5,16–19]. Regular monitoring enables early detection of surface deterioration and supports timely intervention. However, the overall effectiveness of APMS relies heavily on the quality and accuracy of pavement distress data collected [6,12,16,20,21]. Within APMS, the 'Network Inventory' and 'Condition Assessment' components collect and structure key information such as pavement characteristics, traffic data, types of distress, construction history and repair records which are stored and organized in a central 'Database'. This organized dataset supports accurate condition evaluation and informed decision-making regarding maintenance and rehabilitation planning. Ultimately, this information's quality directly impacts the system's ability to ensure performance and safety [4,5,12,16–20,22–24]. Fig. 1 presents the main APMS components and their

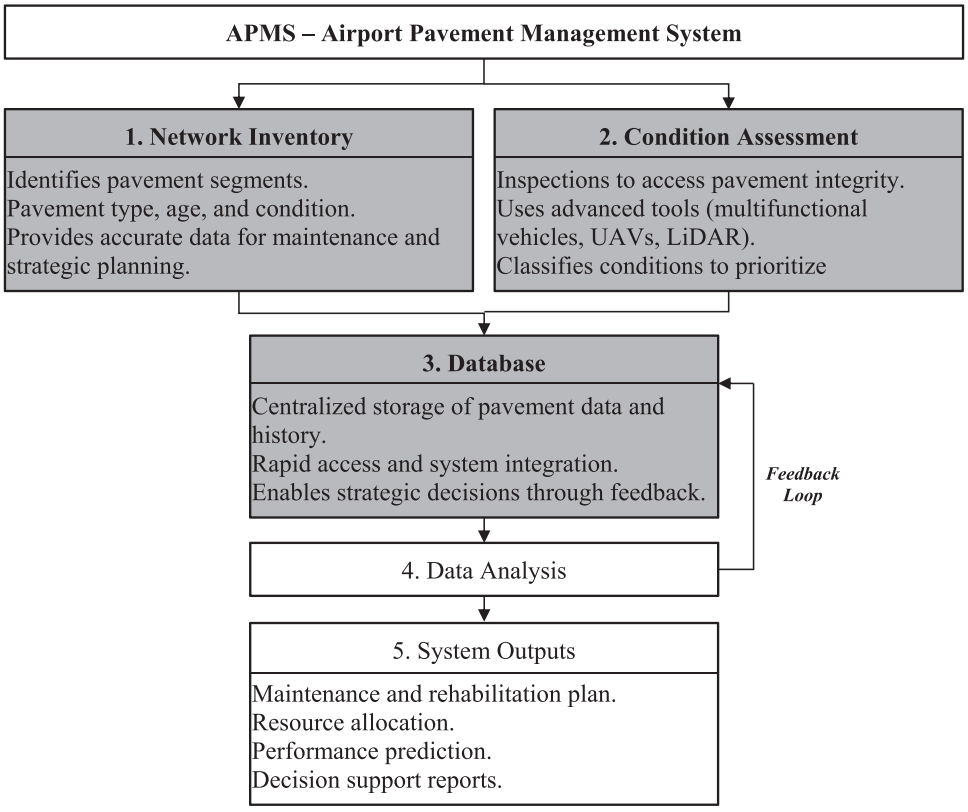

Fig. 1. Main components of an APMS.

interactions.

This study contributes to the development of the 'Network Inventory', 'Condition Assessment', and 'Database' components by improving data collection, organization, and storage processes. By integrating advanced inspection technologies and automation, the study enhances pavement evaluation accuracy and supports more effective maintenance strategies within APMS.

Thanks to ongoing technological advancements, various pavement distress data collection methods have emerged to support APMS. In pavement inspection, automation and real-time data collection are transforming the management of airport pavement assets. The shift from traditional methods, such as on-foot inspections, to multi-functional ground and aerial vehicles represents a significant step toward overcoming operational limitations and workforce constraints. These innovations not only reduce costs but also significantly improve the efficiency of airport pavement management [1,4–6,12,25–27].

Multi-functional ground vehicles use advanced technologies such as GNSS, laser systems, high-resolution optical cameras, and Light Detection and Ranging (LiDAR) to collect pavement data with greater accuracy and effectiveness. These systems are adaptable to road and airport contexts, offering a cost-effective alternative to traditional inspections and enhancing overall pavement management performance [1,13,26,27]. Unmanned Aerial Vehicles (UAVs) have also emerged as a promising solution for inspecting transport infrastructure. Equipped with high-resolution cameras and GNSS, UAVs can collect data with precision. They are particularly effective in generating detailed 3D surface models through Structure from Motion (SfM), allowing the identification of distresses such as cracks and potholes. When integrated with machine learning tools, such as Convolutional Neural Networks (CNN) and other classification algorithms, UAV systems enable automated distress detection, making pavement management more efficient than traditional methods [1,28–32].

Despite limitations, such as battery autonomy, dependency on favorable weather, and regulatory constraints, UAVs offer high operational flexibility. They also present advantages, such as lower costs compared to ground vehicles and traditional inspections, rapid data collection, reduced environmental impact, and enhanced safety for inspection teams [1,29,30,32].

Recent research has further advanced this field by integrating deep learning and AI techniques into pavement inspection systems to improve classification accuracy and reduce manual intervention [1,28–34]. However, many of these approaches prioritize algorithmic performance - typically reporting metrics, such as precision, recall, and IoU (Intersection over Union) - while lacking rigorous, field-based statistical validation. As highlighted in the literature [35–39], there remains a clear need for research that combines automation with robust statistical comparison frameworks capable of evaluating inspection systems beyond controlled or simulated environments.

To respond to this challenge, an innovative inspection method has been under development since 2015 at the Department of Civil Engineering and Architecture of the University of Beira Interior (DECA-UBI). This solution, tested in real operational contexts, is based on a low-cost in-vehicle system equipped with laser scanners, image capture, and geo-referencing systems. It aims to improve the detection and classification of surface distress in airport and road pavements while reinforcing the integration of accurate and structured data into APMS components [1,6,12,13,15,24,40–44].

Expanding on previous work, the comparative statistical study conducted in [6] has been extended and refined to validate the method developed at UBI more comprehensively. The system was tested on the main runway of Amílcar Cabral International Airport, on Sal Island, Cape Verde, designed by the International Civil Aviation Organization (ICAO) code GVAC and International Air Transport Association (IATA) code SID, using data collected with both the in-vehicle and conventional on-foot inspections methods [40]. The dataset used in this study includes distress type, severity, and density values for identical sample units [6,12,13]. A suite of non-parametric statistical tests was applied to compare both methods rigorously, identify systematic discrepancies, and determine areas for enhancement.

This work's primary scientific contribution lies in applying a structured statistical validation framework in a real-world airport environment. Unlike studies based on simulated datasets or visual comparisons [35–38,45], this research presents quantitative evidence - through hypothesis testing, effect size estimation, and correlation analysis - on the degree of agreement between traditional and automated inspections. Furthermore, it identifies biases in severity classification and explores spatial patterns such as autocorrelation, contributing new insights into how inspection methods perform across different runway sections. By addressing this methodological gap, the study enhances the credibility of automated inspection systems and proposes a scalable approach to validate similar technologies in operational contexts. These findings not only reinforce the value of automated inspection in APMS but also support its implementation as a cost-effective and technically reliable alternative to traditional assessment strategies.

The article is structured into five main sections. Section 1 introduces the significance of airport pavement maintenance and outlines the research motivation and objectives. Section 2 describes the statistical methods applied in the study. Section 3 details the case study and presents the statistical analysis. Section 4 discusses the findings, and Section 5 summarizes the conclusions and future directions.

2. Methods

2.1. Analysis framework and sample details

Statistics provides methods for analyzing and interpreting data to effectively understand study samples under conditions of uncertainty [46–48]. In the present study, comparative statistical analysis plays a crucial role in assessing the significance and relevance of a new pavement inspection method and its impact on the study objectives.

To assess the pavement data and compare the inspection methods, the statistical analysis was structured according to the dataset's characteristics. Given the presence of repeated measures (in-vehicle image-based and on-foot inspections on the same sample units), the non-normal variable distributions, and the need to compare independent groups across pavement sections, a combination of non-

parametric methods was adopted. The nparLD method was used to evaluate repeated measures in a factorial design, while the Kruskal-Wallis and Dunn-Bonferroni tests were applied to analyze differences between independent groups. In addition, the Spearman rank correlation was used to assess the association between inspection methods, and autocorrelation analysis was performed to detect potential biases in distress identification. This integrated approach ensured that the statistical tools were properly aligned with both the structure of the data and the objectives of the analysis.

The pavement data analyzed in this study was collected at the Amílcar Cabral International Airport (runway 01–19) by the research team from DECA-UBI, using two inspection methods: the traditional on-foot inspection, with digital alphanumeric data recording and the proposed in-vehicle system, equipped with laser, image capture, and positioning devices. The runway pavement area was divided into sections and sample units according to ASTM D5340–12 [49]. This standard uses a systematic random sampling strategy to select the minimum number of units to be inspected and evaluated in each pavement section to obtain a statistically adequate estimate (95 % confidence) of the section's Pavement Condition Index (PCI).

The statistical comparative analysis was designed to align with the research objectives and variable characteristics, including their type (qualitative or quantitative), data distribution, and sample structure. Other considerations included the quality and quantity of data available, the sampling method used (probabilistic or non-probabilistic), the relationship between samples (independent or paired), and the number of data groups involved in the analysis [6,12,46,47].

To enhance the analysis, the identified distress types were categorized using specific codes: AC for Alligator Cracking, PC for Patching and utility Cuts, RA for Raveling, and WA for Weathering in surface wear-dense mix Asphalt. Severity levels were classified as L (Low), M (Medium), and H (High). Inspections were conducted both on-site, on-foot (f) and using the proposed in-vehicle image-based method (v), with the number of valid sample units represented by n. Therefore, the code AC_Lv refers to low severity alligator cracking density identified during the data collection with the in-vehicle image-based method. By combining distress codes and severity classifications, the study provides a detailed understanding of the pavement condition.

In a previous study on the collected data for pavement distress density on runway 01–19, three types of analyses were explored [6]: descriptive, normality, and comparative. An initial descriptive analysis of the variables was conducted, providing a detailed understanding of the distributions and trends in the data. The normality of the density data, categorized by severity level and type of distress in the 43 inspected sample units, was assessed using the Shapiro-Wilk and Kolmogorov-Smirnov normality tests. The p-values obtained generally indicated non-normality in the distress densities associated with both on-foot and multi-functional ground vehicle inspections (p-value < 0.05). These results confirmed previous indications of severity-level identification and classification limitations during inspections [6,12]. Lima (2016) [40] reported difficulties in identifying low-severity levels of distress from images captured using the in-vehicle image-based solution, particularly for raveling and weathering (surface wear) - dense mix asphalt. Non-validated cases may, therefore, be attributed to these limitations. The comparative analysis in [6] applied the Wilcoxon test to validate the remaining distress-severity pairs and PCI values. Additionally, the *t*-test validated PCI values, while the f-test assessed variance differences. The results indicated that using the in-vehicle image-based inspection method did not significantly influence PCI results, as both the *t*-test (mean comparison) and f-test (variance comparison) produced p-values greater than 0.05.

To build on this previous work, the current study expands the analytical scope by incorporating additional statistical tests. A new variable—pavement section—was introduced, allowing a more detailed examination of how distress type, severity, and density vary across sections and methods. The analysis evaluates the influence of these variables and their interactions.

Given the non-normality of the variables and the observed variation between groups, the nparLD (Non-Parametric Analysis of Longitudinal Data) test was chosen to deal with repeated measures robustly. The Kruskal-Wallis test was used to compare independent groups, followed by the Dunn-Bonferroni test to make multiple comparisons between groups, with p-values adjusted to control for Type I error. Type I error refers to the probability of wrongly rejecting the null hypothesis when it is true, and this adjustment minimizes the probability of concluding that a difference exists between groups when it does not. In addition, the Spearman correlation coefficient was used to assess associations between variables, while the autocorrelation test identified temporal dependencies. The Relative Treatment Effect (RTE) metric was also calculated to aid in interpreting the results [48,50–55].

Hypothesis tests were interpreted at a 5 % significance level, with p-values below 0.05 indicating statistically significant differences between groups or relevant associations between variables. Plots with 95 % confidence intervals were used to provide accurate estimates of data variability and strengthen the conclusions' robustness. This comprehensive statistical approach ensured a rigorous evaluation of the effects and interactions between the variables studied.

Statistical test selection considered the data's non-parametric nature and repeated measures structure. The rationale for using nparLD, Kruskal-Wallis with Dunn-Bonferroni, and Spearman's correlation is presented in the following subsections.

2.1.1. Non-parametric data analysis with nparLD: comparison and relative effect

This approach provides ANOVA-type and Wald-type statistics for each effect. For the present study, the effects of the data collection method, runway section, and the interaction between the method and section were considered. The approach also includes an RTE measure for analysis [54].

Considering the asymmetry in the distribution of each variable (types of pavement distress by severity level), the small sample size, and the presence of missing data, the nparLD test was selected due to its ability to handle longitudinal data consisting of repeated measurements on the same units over time (such as days, months, or years) [51–54,56]. In this study, on-foot and in-vehicle surveys were conducted over several days, allowing for comparing both methods and assessing whether the in-vehicle system could effectively replace the traditional on-foot inspection by analyzing variations within the same sample units.

This test was essential because the data did not satisfy the normality assumptions required for parametric repeated measures tests such as ANOVA (see Fig. 2). Normality tests, specifically the Shapiro-Wilk and Kolmogorov-Smirnov tests, confirmed that the data did

not follow a normal distribution [6]. Each method assessed the same sample units once, justifying the study's consideration of only one repetition per sample unit for both the in-vehicle image-based and on-foot methods. Each sample unit can exhibit multiple types of pavement distress, with each type having up to three severity levels (low, medium, and high) and specific distress densities. The analysis was performed separately for each combination of runway section, distress type, and severity level. Since the methods evaluated the same areas within these sections, the data consists of repeated measures from the same units. This approach ensures consistency across analyses while accounting for the complexity introduced by multiple distress types and severity levels within each sample unit and section.

Fig. 2 summarizes the decision process that guided the selection of the statistical tests. The choice of the nparLD method was based on several key factors: the presence of repeated measures on the same sample units (comparing two inspection methods), a small and unbalanced sample size, and the non-normal distribution of the variables. These conditions make nparLD a robust and reliable option, especially when compared to parametric approaches or linear mixed models. Although mixed models are widely used for repeated measures, they assume normality and homoscedasticity, assumptions that were not met in this study, and tend to perform poorly with small samples [57]. In contrast, the nparLD method provides a statistically sound solution well-suited to the present dataset's characteristics [48,54].

The results of the nparLD test were considered statistically significant if the p-value did not exceed the 5 % significance level (p-value < 0.05), indicating meaningful differences between data collection methods, runway sections, or their interaction. A 95 % confidence interval was used to support the interpretation of the results. Additionally, the analysis of the RTE was included, allowing for a more detailed and accurate comparison between the groups and conditions under evaluation [54].

Overall, the nparLD method enabled a robust non-parametric analysis, ensuring a reliable evaluation of the inspection methods and observed effects while accounting for the structure of repeated measurements and the dataset's characteristics.

2.1.2. Kruskal-Wallis test and Dunn-Bonferroni test

The Kruskal-Wallis test was used to compare the different pavement sections. This is a non-parametric approach employed to assess the existence of significant differences between independent groups and is particularly useful when the data does not follow a normal distribution. The Dunn-Bonferroni test was then used for pairwise comparisons between the sections [54]. Fig. 3 presents the decision process for statistical tests based on data distribution (normal or non-normal), which guided the choice between parametric (ANOVA) and non-parametric (Kruskal-Wallis) tests, as well as subsequent post-hoc analyses, such as Tukey, Bonferroni, or Dunn-Bonferroni tests, depending on the significance results (p-values).

The results of the Kruskal-Wallis test, followed by the Dunn-Bonferroni post hoc test and the Dunn-Bonferroni adjustment for multiple comparisons, were considered statistically significant when the corresponding p-value was below the 5 % significance level (p-value < 0.05). This method ensured the validity of observed group differences while controlling Type I errors. In addition, a 95 % confidence interval was used to improve the results' interpretation and assess the precision of the estimated differences.

The importance of this analysis lies in the fact that different pavement sections may experience different distress processes depending on their specific functions and demands. Factors such as the location of the section, i.e. whether it is a landing or takeoff runway or a taxiway area, and its exposure to traffic play a significant role in influencing variations in wear patterns. Comparing sections is crucial to detecting such variations and planning targeted maintenance actions. It ensures that higher-stress areas receive priority attention while less-stressed sections can be maintained with fewer resources, promoting more efficient management and extending the overall life of the pavement.

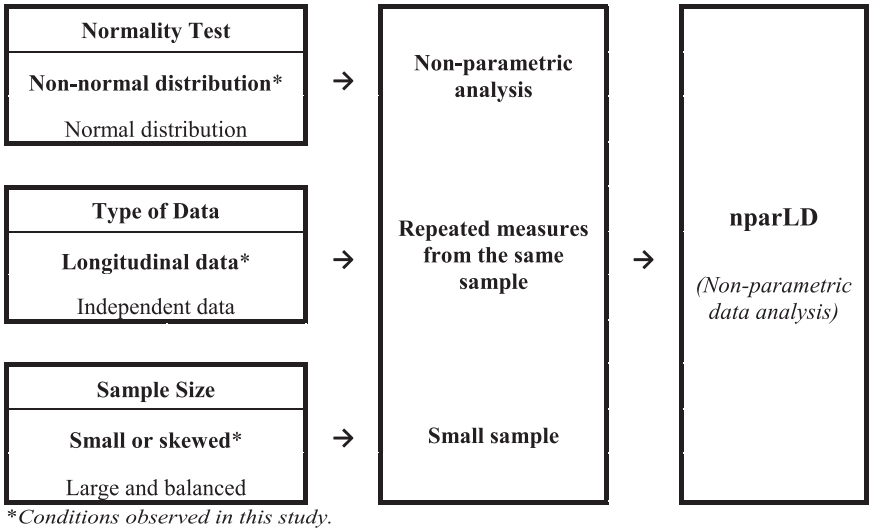

Fig. 2. Decision process to support the use of the nparLD test.

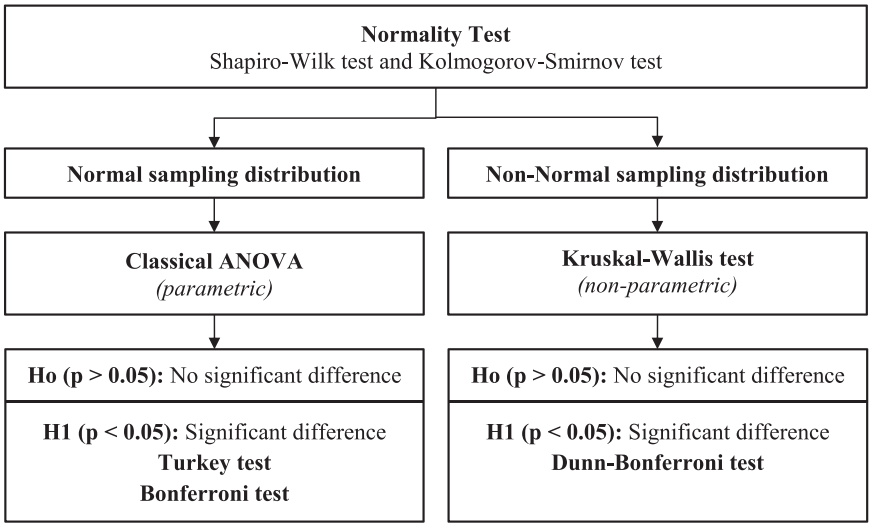

Fig. 3. Decision process to support the use of the Kruskal-Wallis and Dunn-Bonferroni tests.

2.1.3. Correlation and autocorrelation tests

The correlation between the data collection methods (on-foot and with the in-vehicle image-based method) was assessed using Spearman's rank correlation coefficient due to the non-parametric nature of the data [54]. The coefficient r_s was used to assess the strength and direction of the association between the two methods. A value of r_s close to + 1 indicates a strong positive correlation, while a value close to −1 indicates a strong negative correlation. A value close to 0 indicates little or no correlation between the methods.

In addition, an autocorrelation analysis was performed by inspectors to identify potential biases in the detection of pavement distress, ensuring a rigorous evaluation of the agreement between the analyzed methods [55]. The autocorrelation function (ACF) was used to examine the correlation between observations at different lag values. The results are presented in graphs where the autocorrelation coefficient (represented by blue bars) is plotted against the lag number. Confidence intervals (upper and lower limits) are included to indicate the expected range for random autocorrelations. If the coefficient bars extend beyond these confidence limits, this indicates a statistically significant autocorrelation, suggesting dependencies or patterns in the data that may point to bias in the inspection process. If the bars fall within the confidence limits, the autocorrelation is not statistically significant, suggesting that the observations are independent and free from systematic error.

Table 1
Coding and segmentation of GVAC runway 01–19 [6].

Pavement	Code	Description/Comments
Pavement network – Airport	SID/GVAC	SID (IATA), GVAC (ICAO)
Pavement branches	R01	Main runway (01−19)
	TWY	Taxiway
	BER	Shoulders
	APR	Apron
R01 pavement sections	A	900 m measured from end 01 (touchdown area)
	B	1200 m in the central part of the runway
	C	900 m measured from end 19 (touchdown area)
Pavement sampling units – total runway area (segmentation according to ASTM D5340 sample area criteria)	A: 81 sampling units B: 108 sampling units C: 81 sampling units	500 m^2 sampling units (100 m by 5 m) – In-vehicle image-based data collection
Pavement sampling units – sample area for inspection (minimum area to inspect according to ASTM D5340–12)	A: 14 sampling units B: 15 sampling units C: 14 sampling units	500 m^2 sampling units (100 m by 5 m) – On-foot and in-vehicle image-based data collection

3. Case study: Amílcar Cabral International Airport (Cape Verde)

3.1. Framework

Cape Verde's airport system, consisting of seven infrastructures, plays a key role in the economy, particularly in the tourism sector. This highlights the importance of air transport in connecting the islands within the archipelago and with other nations, driving economic development and influencing the daily lives of citizens [15,40]. The study presented in this section focuses on runway 01–19 at Amílcar Cabral International Airport on the island of Sal, Cape Verde, identified by the codes SID (IATA) and GVAC (ICAO). The runway dimensions are 45 m by 3000 m, with a shoulder width of 7.5 m.

For the pavement condition analysis, runway 01–19 at GVAC was divided into 3 sections, and 270 sampling units [15]. Of these, 43 sampling units located in the 3 sections of the runway were inspected, meeting the minimum requirement of ASTM D5340–12 standard [49]. Both the on-foot and the proposed in-vehicle methods were used for data collection. Details of the coding and segmentation are presented in Table 1 and Fig. 4.

It is noteworthy that while all 270 sampling units of the pavement surface of runway 01–19 at GVAC were surveyed using the in-vehicle data collection method, only the 43 sampling units that were inspected by both the on-foot and in-vehicle methods were selected for analysis. Fig. 4 shows the locations of the three runway pavement sections and the selected sampling units. Due to runway access restrictions, imaging data collection for runway 01–19 took place over three days, while the on-foot inspection of the 43 sampling units was completed in three weeks [15,40].

Inspection by the in-vehicle system, using laser scanning, imagery and georeferencing data, has enabled the collection of information that is used to identify pavement surface distress and severity levels in post-processing. During daytime inspections, data can be collected on alligator cracking, bleeding, block cracking, jet blast erosion, joint reflection cracking, longitudinal and transverse cracking, oil spillage, patching and utility cuts, polished aggregate, raveling, surface weathering, shoving of asphalt pavement, and slippage cracking. Night inspections allow the collection of surface texture and depth distress data, such as those associated with rutting, corrugation, depressions, and swelling distress [40,49,58]. Following the inspection, the set of GNSS-based positions and imagery collected by the in-vehicle inspection system was processed for visualization in a Geographic Information System (GIS). The images formed a continuous stream with a spatial resolution of less than 0.003 m per pixel in the central area of the image and reduced resolution towards the edges due to the geometric distortion of the optical system. The GIS visualization interface facilitated assessing and identifying pavement surface distress, determining severity levels, and measuring distress influence areas and lengths. The information generated by the projection of the laser beam over the road surface is interpreted for nighttime data collection. The digitization process achieved an average vertex positioning accuracy of 2 pixels, equivalent to 0.006 m.

Pavement distress was also assessed on foot by a trained inspector walking through the selected sample units, identifying and rating the distress type and severity level according to the ASTM D5340–12 distress catalogue for flexible pavements [49]. Tools such as measuring wheels, chalk, and 3 m and 40 centimeters rulers were used to measure the affected areas, lengths, and depths of the pavement distress. Data was recorded on survey forms and then entered into spreadsheets to calculate the PCI for each sample unit [40,49,58]. On-foot measurements using a measuring wheel provided sub-decimeter accuracy for linear distress quantities. The same trained inspector performed all on-foot inspections to minimize subjectivity and ensure consistency in distress classification. In cases of

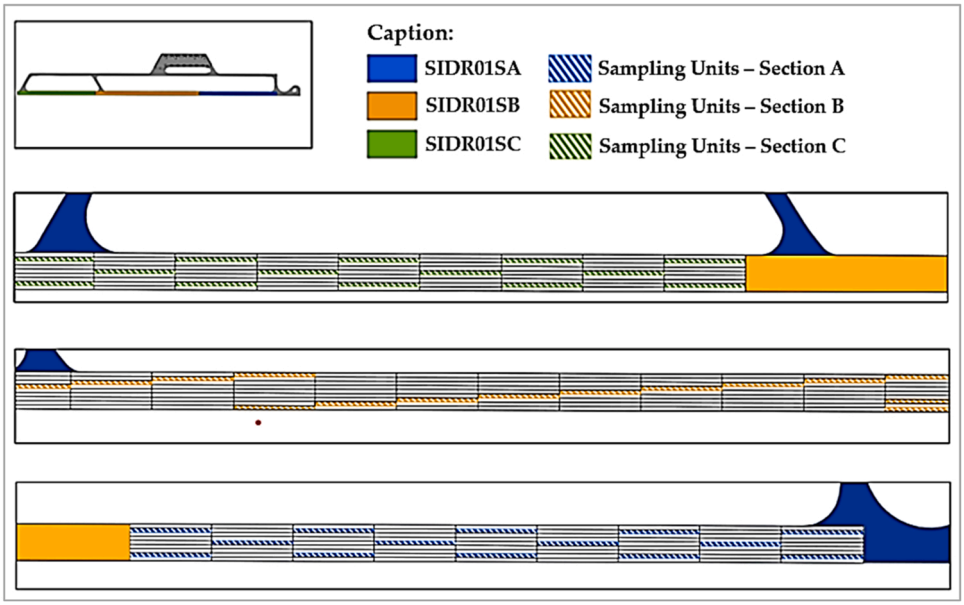

Fig. 4. Segmentation of Amílcar Cabral International Airport runway in sections and sample units [40].

uncertainty regarding severity levels, the inspector revisited the sample units within the same week for verification. This approach, combined with a standardized methodology for data entry and PCI calculation, helped reduce observational and transcription errors, thereby enhancing the overall integrity of the results.

Thus, measuring distress lengths and areas using images through careful raster-to-vector digitization showed greater accuracy than in-situ measurements using a measuring wheel [6,40]. Fig. 5 shows an extract from the GIS visualization of part of sample unit 71 in section A. The distress patching and utility cut patch are clearly visible in this image.

Six types of distress were identified during the on-foot inspection of the 43 sample units: alligator cracking, longitudinal and transverse cracking, patching and utility cuts, raveling, weathering in surface wear and depressions while the in- vehicle inspection identified four types of distress: alligator cracking, patching and utility cuts, raveling, and weathering in surface wear. Four of the six types of distress were detected by both inspection methods. Distresses not identified by the in-vehicle method were depressions and longitudinal and transverse cracks. These distresses exhibited low densities and severity levels, which may have affected identification due to the difficulty of detecting low-severity distresses in images or errors in assigning severity levels. It is worth noting that both inspections and data processing were conducted by the same inspector, thus ensuring the consistency of the results [12,40,44].

A first comparative statistical analysis of the two inspection results was performed and reported in [6]. This analysis consisted of the use of normality tests (Kolmogorov-Smirnov and Shapiro-Wilk tests) to assess data distribution, followed by parametric (*t*-test) and non-parametric (Wilcoxon test) methods to compare distress density data. To enhance this evaluation and address its limitations and challenges, this study employed advanced statistical methods, including nparLD (non-parametric ANOVA), Kruskal-Wallis test, Dunn-Bonferroni test, Spearman correlation, autocorrelation function, and RTE. These methods enable a more detailed analysis of the agreement between the inspection methods and the identification of potential biases in the inspection process. The results of the performed analysis are presented and discussed in the following sections. The statistical software used in this study includes IBM SPSS Statistics 27 (SPSS) [59] and R Statistics 4.0.2 [60]. Additionally, nparLD (version 2.1) for R, a package specifically designed to analyze non-parametric longitudinal data [51,52,56], was used.

3.2. Results

Tables 2a−2c present the descriptive statistical analysis of the variables related to the density of the analyzed distresses, including the mean, standard deviation (SD), median, and interquartile range.

In Tables 2a−2c, it can be observed that, in most cases, the means and standard deviations of the distresses obtained with the two inspection methods are similar. However, notable differences were found for raveling in Section A (RA_Lv: 0.00 - RA_Lf: 4.13; RA_Mv: 5.12 - RA_Mf: 13.46) and Section C (RA_Hv: 18.77 - RA_Hf: 12.86), and for weathering in surface wear in Section C (WA_Hv: 20.32 - WA_Hf: 13.79). The medians also revealed differences in some cases in Section A (WA_Mv: 0.00 - WA_Mf: 12.00; WA_Hv: 27.31 - WA_Hf: 0.00; and AC_Lv: 14.68 - AC_Lf: 7.60) and Section C (WA_Hv: 17.39 - WA_Hf: 13.75). The number of valid samples varied more significantly in Sections A and C, while Section B showed less wear.

The results of the ANOVA-type and Wald-type statistics for each effect, namely inspection method, section, and interaction method-section, are detailed in Table 3. This table provides a comprehensive view of the statistical analysis of distress levels by severity and data collection method. Significant effects related to the data collection method on the density of distress were observed, except for patching and utility cuts of high severity (p-value = 0.061), raveling of medium and high severity (p-value = 0.680 and p-value = 0.582), and weathering of surface wear of medium severity (p-value = 0.530). The pavement section had significant effects for most distresses, except medium-severity patching and utility cuts (p-value = 0.663) and medium-severity raveling (p-value = 0.525). The interaction method-section showed no significant effects for patching and utility cuts of medium severity (p-value = 0.687), raveling of medium severity (p-value = 0.548), and raveling of high severity (p-value = 0.881).

The mean ranks, Relative Treatment Effects (RTE), and p-values for each type of distress and section, based on the comparison between the inspection methods, are presented in Table 4. All distresses were validated except for the following cases: for patching and utility cuts low severity in Section A (p-value = 0.003), medium severity in Section B (p-value = 0.003), and medium and high severity

Fig. 5. GIS visualization of part of sample unit 71 with patching and utility cuts distress.

Table 2a
Descriptive statistical analysis of pavement distress density (Section A).

Code	Section A		
	n	Mean ± SD	Median (1st quartile; 3rd quartile)
AC_Lv	03	12.33 ± 11.34	14.68 (7.34; 18.50)
AC_Lf	04	12.85 ± 17.14	7.60 (0.00; 25.70)
AC_Mv	03	14.62 ± 5.98	16.21 (12.10; 17.93)
AC_Mf	04	16.25 ± 10.19	11.55 (10.70; 21.80)
AC_Hv	03	0.00 ± 0.00	0.00 (0.00; 0.00)
AC_Hf	04	0.00 ± 0.00	0.00 (0.00; 0.00)
PC_Lv	14	0.29 ± 1.10	0.00 (0.00; 0.00)
PC_Lf	14	0.54 ± 0.89	0.11 (0.00; 0.80)
PC_Mv	14	0.50 ± 0.54	0.30 (0.00; 0.86)
PC_Mf	14	0.25 ± 0.47	0.00 (0.00; 0.24)
PC_Hv	14	1.31 ± 0.55	1.30 (1.00; 1.60)
PC_Hf	14	1.12 ± 0.63	1.23 (0.76; 1.60)
RA_Lv	11	0.00 ± 0.00	0.00 (0.00; 0.00)
RA_Lf	05	4.13 ± 6.28	1.80 (0.00; 3.84)
RA_Mv	11	5.12 ± 9.87	0.00 (0.00; 6.07)
RA_Mf	05	13.46 ± 19.51	0.00 (0.00; 24.58)
RA_Hv	11	4.34 ± 5.72	2.03 (0.00; 6.50)
RA_Hf	05	5.28 ± 11.81	0.00 (0.00; 0.00)
WA_Lv	12	4.52 ± 10.93	0.00 (0.00; 0.00)
WA_Lf	13	13.84 ± 18.88	0.00 (0.00; 22.40)
WA_Mv	12	4.25 ± 9.06	0.00 (0.00; 4.05)
WA_Mf	13	23.45 ± 25.33	12.00 (0.00; 40.20)
WA_Hv	12	30.86 ± 23.50	27.31 (21.78; 38.40)
WA_Hf	13	11.67 ± 14.80	0.00 (0.00; 19.60)

Note: AC – Alligator cracking; PC – Patching and utility cuts; RA – Raveling; WA – Weathering in surface wear (dense mix asphalt); L – Low; M – Medium; H – High; f – On-foot method; v – In-vehicle image-based method; n - Number of valid samples

Table 2b
Descriptive statistical analysis of pavement distress density (Section B).

Code	Section B		
	n	Mean ± SD	Median (1st quartile; 3rd quartile)
AC_Lv	02	5.06 ± 7.15	5.06 (0.00; 10.11)
AC_Lf	04	8.61 ± 11.91	4.60 (0.00; 17.22)
AC_Mv	02	1.31 ± 1.86	1.31 (0.00; 2.63)
AC_Mf	04	3.41 ± 3.99	3.03 (0.00; 6.83)
AC_Hv	02	0.00 ± 0.00	0.00 (0.00; 0.00)
AC_Hf	04	0.70 ± 1.40	0.00 (0.00; 1.40)
PC_Lv	15	0.00 ± 0.00	0.00 (0.00; 0.00)
PC_Lf	15	5.76 ± 11.92	0.00 (0.00; 0.00)
PC_Mv	15	5.94 ± 10.67	0.20 (0.00; 7.96)
PC_Mf	15	2.00 ± 7.74	0.00 (0.00; 0.00)
PC_Hv	15	0.66 ± 0.56	0.60 (0.40; 0.80)
PC_Hf	15	0.87 ± 0.59	0.64 (0.60; 0.91)
RA_Lv	13	0.00 ± 0.00	0.00 (0.00; 0.00)
RA_Lf	12	0.80 ± 2.79	0.00 (0.00; 0.00)
RA_Mv	13	1.60 ± 3.18	0.00 (0.00; 1.15)
RA_Mf	12	2.37 ± 8.23	0.00 (0.00; 0.00)
RA_Hv	13	22.11 ± 16.73	18.60 (9.83; 27.73)
RA_Hf	12	22.69 ± 18.77	18.33 (14.32; 28.35)
WA_Lv	15	0.00 ± 0.00	0.00 (0.00; 0.00)
WA_Lf	14	0.07 ± 0.26	0.00 (0.00; 0.00)
WA_Mv	15	4.94 ± 8.29	0.00 (0.00; 6.39)
WA_Mf	14	1.59 ± 4.87	0.00 (0.00; 0.00)
WA_Hv	15	26.10 ± 12.59	23.40 (22.11; 32.66)
WA_Hf	14	26.45 ± 16.62	21.16 (15.99; 41.04)

Note: AC – Alligator cracking; PC – Patching and utility cuts; RA – Raveling; WA – Weathering in surface wear (dense mix asphalt); L – Low; M – Medium; H – High; f – On-foot method; v – In-vehicle image-based method; n - Number of valid samples.

in Section C (p-value = 0.002 and p-value < 0.001); for raveling, low severity in Section A (p-value = 0.015); and for weathering in surface wear, medium and high severity in Section A (p-value < 0.001) and high severity in Section C (p-value = 0.024).

Tables 5 and 6 summarize the outcomes of the Kruskal-Wallis and Dunn-Bonferroni tests, which assess differences in distress density by section.

Table 2c
Descriptive statistical analysis of pavement distress density (Section C).

Code	Section C		
	n	Mean ± SD	Median (1st quartile; 3rd quartile)
AC_Lv	04	0.00 ± 0.00	0.00 (0.00; 0.00)
AC_Lf	00	-	-
AC_Mv	04	12.35 ± 5.42	12.31 (8.02; 16.67)
AC_Mf	00	-	-
AC_Hv	04	0.00 ± 0.00	0.00 (0.00; 0.00)
AC_Hf	00	-	-
PC_Lv	14	0.00 ± 0.00	0.00 (0.00; 0.00)
PC_Lf	14	0.00 ± 0.00	0.00 (0.00; 0.00)
PC_Mv	14	0.37 ± 0.43	0.30 (0.00; 0.60)
PC_Mf	14	0.75 ± 2.80	0.00 (0.00; 0.00)
PC_Hv	14	1.52 ± 2.00	0.98 (0.50; 1.28)
PC_Hf	14	3.85 ± 7.12	1.40 (1.20; 2.40)
RA_Lv	11	0.00 ± 0.00	0.00 (0.00; 0.00)
RA_Lf	14	0.00 ± 0.00	0.00 (0.00; 0.00)
RA_Mv	11	3.76 ± 8.39	0.00 (0.00; 0.00)
RA_Mf	14	1.32 ± 3.48	0.00 (0.00; 0.00)
RA_Hv	11	18.77 ± 17.32	12.44 (4.87; 31.67)
RA_Hf	14	12.86 ± 1.10	9.85 (7.55; 12.24)
WA_Lv	12	2.49 ± 8.64	0.00 (0.00; 0.00)
WA_Lf	12	2.07 ± 5.91	0.00 (0.00; 0.00)
WA_Mv	12	1.28 ± 4.43	0.00 (0.00; 0.00)
WA_Mf	12	0.77 ± 2.65	0.00 (0.00; 0.00)
WA_Hv	12	20.32 ± 15.52	17.39 (10.36; 30.60)
WA_Hf	12	13.79 ± 7.96	13.75 (10.24; 16.98)

Note: AC – Alligator cracking; PC – Patching and utility cuts; RA – Raveling; WA – Weathering in surface wear (dense mix asphalt); L – Low; M – Medium; H – High; f – On-foot method; v – In-vehicle image-based method; n - Number of valid samples.

Table 3
Effects of the inspection method (in-vehicle vs. on-foot), section (A, B, and C), and interaction method–section on pavement distress density (nparLD p-value).

Type of pavement distress	Inspection method	Section	Method-section interaction
AC_L	< 0.001	0.001	0.001
AC_M	< 0.001	0.001	0.001
AC_H	< 0.001	0.001	0.001
PC_L	< 0.001	0.001	0.001
PC_M	< 0.001	0.663	0.687
PC_H	0.061	< 0.001	0.004
RA_L	0.008	0.031	0.031
RA_M	0.680	0.525	0.548
RA_H	0.582	0.002	0.881
WA_L	< 0.001	0.048	0.049
WA_M	0.530	0.006	0.003
WA_H	< 0.001	0.048	0.049

Note: AC – Alligator cracking; PC – Patching and utility cuts; RA – Raveling; WA – Weathering in surface wear (dense mix asphalt); L – Low; M – Medium; H – High.

The Kruskal-Wallis analysis (Table 5) revealed statistically significant differences for most types of distress identified through the traditional on-foot inspection method. These include medium-severity alligator cracking (p-value = 0.020); patching and utility cuts of low (p-value = 0.017) and high severity (p-value = 0.008); raveling of low (p-value = 0.003) and high severity (p-value = 0.031); and weathering in surface wear of low (p-value = 0.026), medium (p-value = 0.002), and high severity (p-value = 0.028). In contrast, the in-vehicle image-based inspection method showed statistically significant differences in only two cases: high-severity patching and utility cuts (p-value = 0.007) and high-severity raveling (p-value = 0.015).

The Dunn-Bonferroni test for pairwise section comparisons (Table 6) showed statistically significant differences between sections A-B (8 cases), A-C (3 cases), and C-B (1 case).

Table 7 presents the statistical results of Spearman's correlation coefficients and the corresponding p-values for the observed correlations. Significant correlations were found for the following distresses: alligator cracking of medium severity (p-value = 0.005), patching and utility cuts of low and high severity levels (p-value = 0.049 and p-value = 0.014), high severity raveling (p-value = 0.003), and weathering in surface wear of high severity (p-value = 0.012).

Low-severity alligator cracking (p-value = 0.054) was close to the statistical threshold. The remaining distresses did not show significant correlations. In particular, the Spearman correlation coefficients for medium-severity patching and utility cuts ($r_s = 0.096$)

Table 4
Analysis of inspection methods by section: average ranks, p-values, and RTE - (nparLD).

Type of pavement distress	Section A			Section B			Section C		
	Average Ranks	RTE	p-value	Average Ranks	RTE	p-value	Average Ranks	RTE	p-value
AC_Lv	4.000	0.500	1.000	3.500	0.500	1.000	14.500	0.500	1.000
AC_Lf	4.000	0.500		3.500	0.500		14.500	0.500	
AC_Mv	4.000	0.500	1.000	3.000	0.417	0.601	14.500	0.500	1.000
AC_Mf	4.000	0.500		3.750	0.542		14.500	0.500	
AC_Hv	4.000	0.500	1.000	3.000	0.417	0.317	14.500	0.500	1.000
AC_Hf	4.000	0.500		3.750	0.542		14.500	0.500	
PC_Lv	11.750	0.402	**0.003**	14.400	0.450	0.062	14.500	0.500	1.000
PC_Lf	17.250	0.598		17.000	0.550		14.500	0.500	
PC_Mv	16.500	0.571	0.098	18.800	0.610	**0.003**	17.714	0.615	**0.002**
PC_Mf	12.500	0.428		12.200	0.390		11.285	0.385	
PC_Hv	15.643	0.541	0.354	13.633	0.438	0.192	11.071	0.377	**< 0.001**
PC_Hf	13.357	0.459		17.367	0.562		17.928	0.622	
RA_Lv	7.000	0.406	**0.015**	12.500	0.480	0.317	13.000	0.500	1.000
RA_Lf	11.800	0.706		13.542	0.522		13.000	0.500	
RA_Mv	8.136	0.477	0.464	14.192	0.548	0.241	13.454	0.518	0.710
RA_Mf	9.300	0.550		11.708	0.448		12.643	0.486	
RA_Hv	9.273	0.548	0.246	13.231	0.509	0.862	14.454	0.558	0.289
RA_Hf	6.800	0.394		12.750	0.490		11.857	0.454	
WA_Lv	11.083	0.423	0.118	14.500	0.483	0.317	12.083	0.483	0.374
WA_Lf	14.769	0.571		15.536	0.518		12.917	0.517	
WA_Mv	10.042	0.382	**< 0.001**	17.133	0.573	0.068	12.542	0.502	0.955
WA_Mf	15.731	0.609		12.714	0.421		12.458	0.498	
WA_Hv	16.917	0.657	**< 0.001**	15.800	0.527	0.581	14.500	0.583	**0.024**
WA_Hf	9.385	0.355		14.143	0.470		10.500	0.417	

Note: AC – Alligator cracking; PC – Patching and utility cuts; RA – Raveling; WA – Weathering in surface wear (dense mix asphalt); L – Low; M – Medium; H – High; f – On-foot method; v – In-vehicle image-based method.

Table 5
Results of the Kruskal-Wallis test for distress density by section (A, B, and C).

Type of pavement distress	Kruskal-Wallis test			
	Section A	Section B	Section C	p-value
	Average Ranks	Average Ranks	Average Ranks	
AC_Lv	6.83	5.25	3.50	0.164
AC_Lf	4.75	4.25	-	0.758
AC_Mv	6.67	1.50	5.50	0.105
AC_Mf	6.50	2.50	-	**0.020**
AC_Hv	5.00	5.00	5.00	1.000
AC_Hf	4.00	5.00	-	0.317
PC_Lv	23.04	21.50	21.50	0.355
PC_Lf	27.00	22.00	17.00	**0.017**
PC_Mv	22.46	22.47	21.04	0.935
PC_Mf	24.86	20.60	20.64	0.228
PC_Hv	29.39	14.63	22.50	**0.007**
PC_Hf	21.82	15.07	29.61	**0.008**
RA_Lv	18.00	18.00	18.00	1.000
RA_Lf	23.20	15.33	14.00	**0.003**
RA_Mv	19.64	17.69	16.73	0.695
RA_Mf	20.10	14.88	15.50	0.220
RA_Hv	10.82	22.46	19.91	**0.015**
RA_Hf	7.80	20.33	15.21	**0.031**
WA_Lv	21.75	18.50	20.13	0.280
WA_Lf	25.04	16.61	18.50	**0.026**
WA_Mv	19.71	23.13	16.38	0.155
WA_Mf	27.19	16.86	15.88	**0.002**
WA_Hv	23.00	21.13	15.58	0.249
WA_Hf	15.62	26.43	17.25	**0.028**

Note: AC – Alligator cracking; PC – Patching and utility cuts; RA – Raveling; WA – Weathering in surface wear (dense mix asphalt); L – Low; M – Medium; H – High; f – On-foot method; v – In-vehicle image-based method.

and for medium-severity weathering in surface wear ($r_s = 0.194$) indicate a very weak relationship.

Of the distresses subjected to autocorrelation analysis, only raveling (RA_H) and weathering in surface wear (WA_H) - both at the high severity level and identified via the traditional on-foot method - showed statistically significant autocorrelation. Figs. 6 to 9

Table 6
Results of the Dunn-Bonferroni test for pairwise section comparison (A, B, and C).

Type of pavement distress	Dunn-Bonferroni test		
	p-value		
	Section A-C	Section A-B	Section C-B
AC_Lv	-	-	-
AC_Lf	-	-	-
AC_Mv	-	-	-
AC_Mf	-	**0.020**	-
AC_Hv	-	-	-
AC_Hf	-	-	-
PC_Lv	-	-	-
PC_Lf	**0.013**	0.443	0.443
PC_Mv	-	-	-
PC_Mf	-	-	-
PC_Hv	0.437	**0.005**	0.274
PC_Hf	0.300	0.440	**0.005**
RA_Lv	-	-	-
RA_Lf	**0.003**	**0.016**	1.000
RA_Mv	-	-	-
RA_Mf	-	-	-
RA_Hv	0.109	**0.016**	1.000
RA_Hf	0.349	**0.028**	0.453
WA_Lv	-	-	-
WA_Lf	0.157	**0.028**	1.000
WA_Mv	-	-	-
WA_Mf	**0.005**	**0.009**	1.000
WA_Hv	-	-	-
WA_Hf	1.000	**0.040**	0.118

Note: AC – Alligator cracking; PC – Patching and utility cuts; RA – Raveling; WA – Weathering in surface wear (dense mix asphalt); L – Low; M – Medium; H – High; f – On-foot method; v – In-vehicle image-based method.

Table 7
Spearman's rank correlation coefficient and p-value for the relationship between variables.

Type of pavement distress	n	Spearman's rank correlation coefficient (r_s)	p-value
AC_Lv - AC_Lf	05	0.872	0.054
AC_Mv - AC_Mf	05	0.975	**0.005**
AC_Hv - AC_Hf	05	-	-
PC_Lv - PC_Lf	43	0.302	**0.049**
PC_Mv - PC_Mf	43	0.096	0.542
PC_Hv - PC_Hf	43	0.371	**0.014**
RA_Lv - RA_Lf	27	-	-
RA_Mv - RA_Mf	27	0.273	0.168
RA_Hv - RA_Hf	27	0.554	**0.003**
WA_Lv - WA_Lf	37	0.308	0.063
WA_Mv - WA_Mf	37	0.194	0.251
WA_Hv - WA_Hf	37	0.408	**0.012**

Note: AC – Alligator cracking; PC – Patching and utility cuts; RA – Raveling; WA – Weathering in surface wear (dense mix asphalt); L – Low; M – Medium; H – High; f – On-foot method; v – In-vehicle image-based method; n - Number of valid samples.

illustrate the corresponding results for these two cases, which were assessed using both inspection methods. Significant positive autocorrelation at lag 1 was observed exclusively with the on-foot method, suggesting a potential spatial pattern or classification bias between successive sampling units. In contrast, the in-vehicle image-based method did not show statistically significant autocorrelation at any lag, indicating a more consistent and spatially independent process of distress assessment.

4. Discussion of results

Similarities in the means and standard deviations of the two inspection methods, as presented in Tables 2a–2c, indicate a general level of consistency and precision between the approaches. However, the significant differences observed in raveling and weathering of surface wear in Sections A and C suggest that the proposed in-vehicle image-based method may tend to overestimate severity levels. In contrast, Section B exhibits lower wear levels than Sections A and C, highlighting the influence of aircraft traffic intensity on pavement deterioration and reinforcing the importance of considering each section's specific usage conditions when evaluating the inspection methods' performance. Although the medians are generally consistent, certain discrepancies suggest potential challenges in

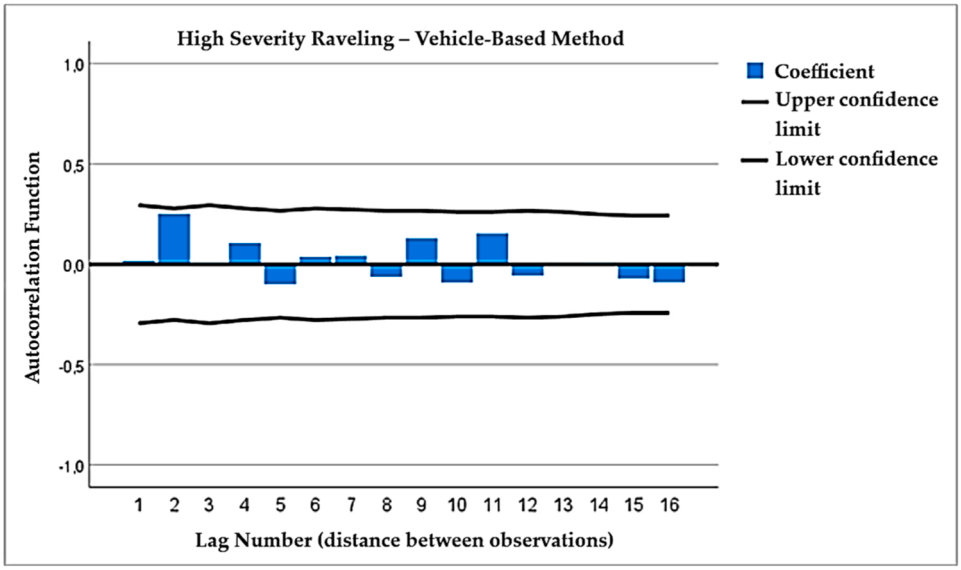

Fig. 6. Autocorrelation chart for high severity raveling (RA_H) – In-vehicle image-based method.

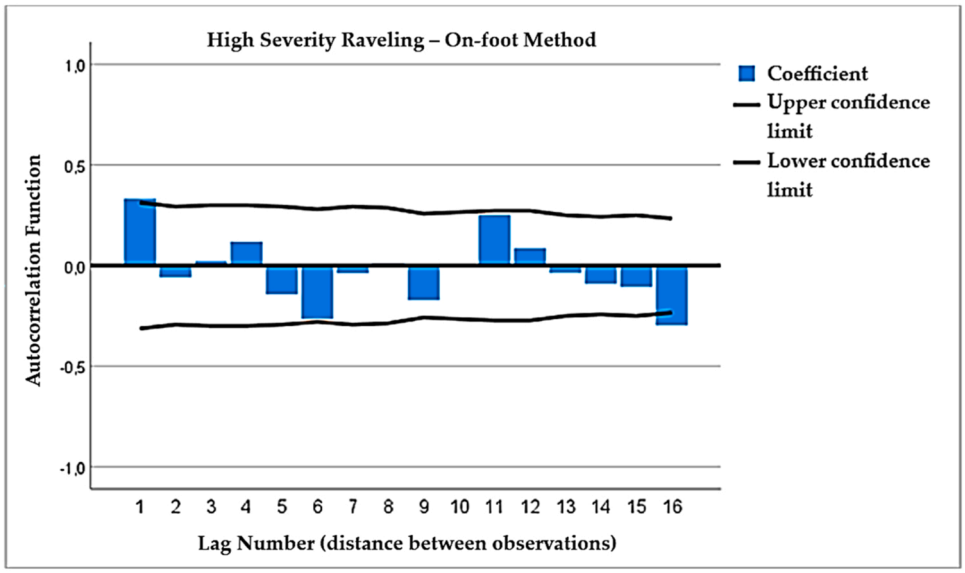

Fig. 7. Autocorrelation chart for high severity raveling (RA_H) – On-foot method.

accurately assigning severity levels. Furthermore, differences in the number of valid samples may reflect inconsistencies in pavement distress identification.

In Table 3, the lack of statistical significance suggests that particular pavement distresses, including high-severity patching and utility cuts (PC_H), as well as medium- and high-severity raveling (RA_M and RA_H), and medium-severity weathering of surface wear (WA_M), exhibit consistent behavior across the pavement, regardless of the data collection method used. This implies that the on-foot and the in-vehicle data collection methods identify and measure these distresses similarly, with no significant differences in the results. Therefore, the proposed in-vehicle image-based method is validated as reliable as the on-foot method for these types of distress and severity levels. However, the proposed in-vehicle method was not validated for the other types of distress, particularly for low-severity levels. Significant differences were found compared to the traditional on-foot method. Most low-severity distresses showed very low or non-existent densities, except for weathering of surface wear (WA_Lf) in Section A during the on-foot data collection. In Section C, low-severity distresses were almost entirely absent for both methods. This indicates that while the in-vehicle image-based method is effective at identifying more severe distresses, its ability to assess low-severity distresses is compromised not only by the low density of such events but also by the spatial resolution of the collected images, which may limit the accurate identification of these distresses.

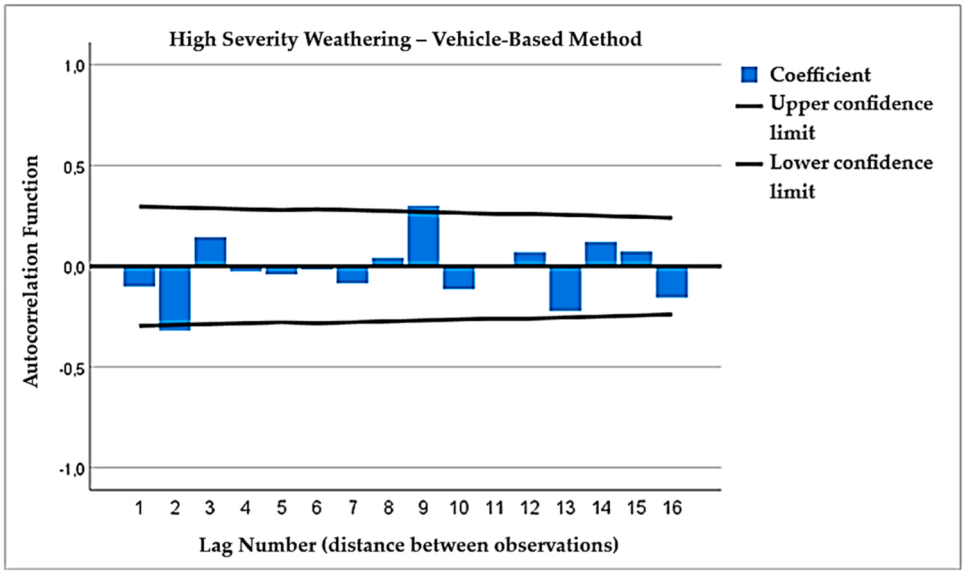

Fig. 8. Autocorrelation chart for weathering in surface wear of high severity (WA_H) – In-vehicle image-based method.

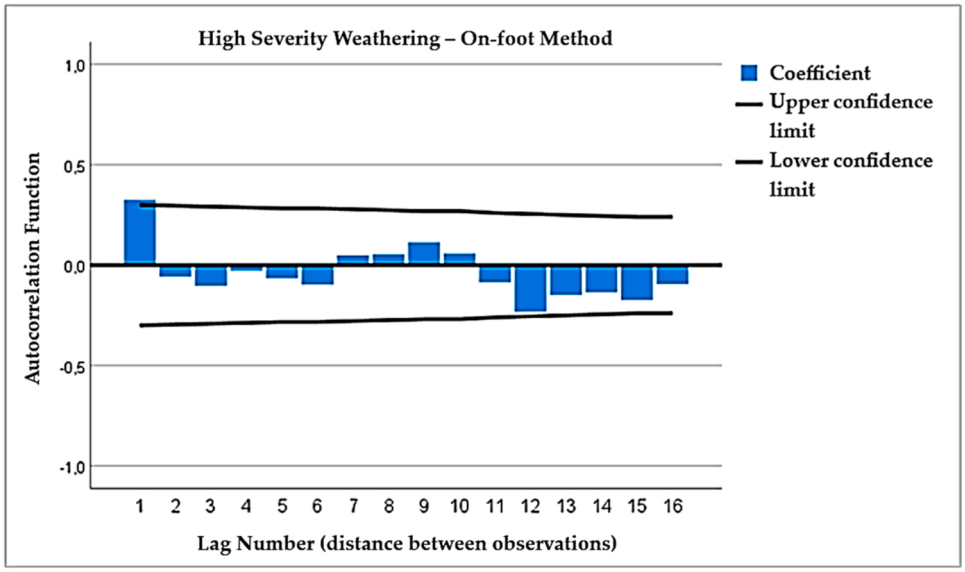

Fig. 9. Autocorrelation chart for weathering in surface wear of high severity (WA_H) – On-foot method.

The sparse distribution of low-severity distresses may also contribute to the variability observed between the methods, making it challenging to establish consistent detection patterns.

Nevertheless, these discrepancies, particularly at low severity levels, were limited and did not substantially impact the overall PCI or compromise the proposed method's statistical validation. This suggests that, despite localized differences, both approaches yield consistent results in assessing the most structurally relevant types of pavement distress.

The analysis of pavement sections further highlights the influence of section location on the distress distribution, except for medium-severity patching and utility cuts (PC_M) and medium-severity raveling (RA_M). This indicates that, in most cases, the location of the sections significantly influences the pavement distress patterns, showing that different areas of the pavement have significant variations in distress conditions. This is likely related to each runway section's distinct functions. Sections A and C are primarily associated with aircraft takeoffs and landings, which involve heavier loads and greater impact forces leading to increased wear and distress. Conversely, Section B, located between these two, experiences comparatively less impact and loading, potentially resulting in less severe distress. However, for PC_M and RA_M, distress patterns appear more uniform across all three sections, suggesting that these specific types of distress are less influenced by section location on the pavement.

The method-section interaction analysis shows no significant effects for certain cases, namely for medium-severity patching and utility cuts (PC_M), medium-severity raveling (RA_M), and high-severity raveling (RA_H). This suggests that, in these cases, the combination of the data collection method and the pavement section does not significantly affect pavement distress density. These specific types of distress exhibit consistent patterns across sections and methods, with little variation in results, regardless of how or where the data collection is conducted.

It is noteworthy that the cases with no significant effect are mainly medium- and high-severity distresses. As distress severity increases, the differences between methods and sections become less pronounced, possibly because high-severity distress is more visible, easier to identify, and more consistently recognized.

In Table 4, all types of distress were validated, indicating the absence of statistically significant differences between the results obtained by the on-foot and in-vehicle methods. However, in some cases, the in-vehicle method was not validated for low-severity distress, suggesting the possibility of significant differences in assessing this severity level.

The results of the Kruskal-Wallis test, presented in Table 5, show statistically significant differences for most of the distress types identified through the traditional on-foot inspection method. Most comparisons did not yield statistically significant results for the distresses identified using the in-vehicle image-based inspection method. The exceptions were two cases, PC_Hv and RA_Hv, where the in-vehicle data collection method detected significant variations in distress, particularly at higher severity levels. This suggests that these distresses' increased visibility and severity facilitated their identification using the in-vehicle method.

The results of the Dunn-Bonferroni test, presented in Table 6, for pairwise comparisons of sections showed statistically significant differences primarily between Sections A-B, followed by A-C and C-B. These results suggest that Sections A and B exhibit different distress characteristics, which could be explained by factors such as traffic intensity or different uses of these areas. Sections A and C, which correspond to the landing and takeoff areas, experience intense wear due to the high impact of aircraft. As previously explained, Section B, less exposed to these extreme conditions, exhibits more uniform distresses due to the lower intensity of applied loads, explaining the observed differences. This suggests that, despite heavy air traffic in both sections, the dynamic forces associated with takeoff and landing impact the pavement differently in Sections A and C compared to Section B. In the context of the GVAC, greater attention should be given to sections A and C due to the severe mechanical stress experienced in these areas. At the same time, Section B, which is less degraded, requires a more targeted and preventive maintenance strategy.

A correlation analysis of the variables in Table 7 was performed using the on-foot and in-vehicle image-based inspection methods. Statistical results indicate that medium-severity alligator cracking, low- and high-severity patching and utility cuts, high-severity raveling, and high-severity weathering in surface wear exhibit statistically significant correlations. This finding suggests that both methods produce similar results in identifying and measuring these specific types of distress, as evidenced by Spearman correlation coefficients that significantly differ from zero. Some types of distress had p-values slightly above 0.05, indicating that the correlation between the data collection methods was not statistically significant. For example, low-severity alligator cracking (p-value = 0.054) is close to the threshold, suggesting some consistency between methods. However, further analysis is needed to confirm this trend using a larger dataset. Additionally, high-severity weathering in surface wear (p-value = 0.063) suggests potential differences between the methods. The differences between methods were even less pronounced for the remaining types of distress, suggesting that these distresses are less sensitive to the data collection method. This may indicate greater variability or inconsistency in the results between methods. However, it is important to note that the first two cases in Table 7, low- (p-value = 0.054) and medium-severity (p-value = 0.005) alligator cracking, are based on a very small sample size (n = 5). While the correlations appear strong, the limited sample size introduces an element of subjectivity that requires caution when interpreting these results. Further analysis with a larger dataset is required to validate these findings and reduce potential variability.

Finally, the autocorrelation analysis of raveling and weathering in surface wear revealed a tendency for the inspector to correlate the measurements of a given sample unit with those of the previous one during on-foot data collection. This trend was not observed in the data collected using the in-vehicle system, suggesting that the in-vehicle image-based method may help mitigate such bias in distress identification.

5. Conclusions and future work

A well-functioning Pavement Management System has been identified as a vital strategy for pavement maintenance. Accurate and reliable pavement condition data is critical to the system's proper functioning. The statistical approach presented, based on non-parametric hypothesis tests such as nparLD, RTE, Dunn-Bonferroni, and Kruskal-Wallis, along with other comparative analysis methods, proved to be an effective methodology for evaluating and identifying improvements in innovative pavement inspection methods. This approach consistently demonstrated its ability to assess the potential of the proposed in-vehicle image-based method, enabling the accurate identification of relevant patterns. It also provided a robust basis for subsequent analysis, providing reliable quantitative support for the evaluation, validating performance where applicable, and identifying areas for improvement in cases where validation was not achieved.

In general, the statistical analysis comparing the on-foot and in-vehicle image-based inspection methods shows no significant differences, indicating the reliability of both approaches. However, it also reveals shortcomings in assigning severity levels using both methods, especially at medium- and high-severity levels. Specifically, discrepancies are observed in the density values. In some cases, the medium-severity levels recorded using the on-foot method were greater than those recorded for high-severity levels. In contrast, the opposite trend was found using the in-vehicle method. This inconsistency suggests possible inversions in ranking severity levels between the two methods.

The comparative statistical analysis validates all cases of alligator cracking and demonstrates reliable performance in identifying

distress and severity levels. However, it shows limitations in detecting low severity levels, particularly for raveling and weathering in surface wear distress.

A notable trend was observed during traditional on-foot data collection, where inspectors tended to introduce bias when identifying raveling and weathering in surface wear distresses at high severity levels. While this observation may raise concerns, it does not affect the proposed method, which has been shown to mitigate such bias. This is primarily because the images captured during in-vehicle inspections are processed in a controlled environment, allowing the reassessment of distresses under identical conditions to those in which they were originally recorded. This approach not only ensures greater consistency, repeatability and objectivity but also minimizes the risk of bias introduced by inspectors during field evaluations, highlighting the robustness and reliability of the in-vehicle system and semi-automatic image processing technology.

Additionally, studying pavement sections is essential for understanding the varying effects of distress processes. By focusing on each pavement section's specific functions and usage intensity, the results confirm significant differences in distress levels, supporting the development of effective pavement management strategies and more efficient resource allocation. Ultimately, this contributes to extending the lifespan of airport pavements and improving operational safety. Methods such as RTE (Ranked Treatment Effects) provide a detailed assessment of pavement conditions, validating these differences and enabling targeted interventions.

The authors conclude that the proposed in-vehicle image-based inspection method accurately identified medium and high-severity distresses. However, limitations were found in the identification of low-severity distress, particularly in raveling and weathering in surface wear. These limitations are primarily attributed to these distress types' sparse occurrence and subtle nature, which present challenges in establishing consistent identification patterns. Targeted improvements to the in-vehicle image-based inspection system are proposed to mitigate these limitations. Upgrading the imaging equipment with higher-resolution cameras will increase spatial resolution, reduce distortion, and improve the detection of minor surface irregularities. Furthermore, adding a second camera dedicated to capturing pavement roughness and minor deformations will provide greater clarity and detail. This enhancement aims to reduce video compression losses and increase sensitivity to subtle surface variations. In addition, the authors emphasize the importance of inspector training to ensure accurate and consistent identification and classification of severity levels during image assessment. Inspector expertise may also influence the results of the comparative statistical analysis.

Compared to traditional on-foot inspections, the validated in-vehicle system, equipped with imaging, laser, and GPS/GNSS devices, stands out for reducing the time required to collect pavement distress information and enabling continuous assessments across the entire pavement surface. The innovative inspection method represents a significant advancement in the field of airport pavement management, and the application of robust statistical analysis, including non-parametric hypothesis testing, has proven essential for in-depth validation and identifying potential improvements.

Further exploration of the proposed inspection method in different airport contexts, ranging from small and regional airports to large international hubs, can help validate its adaptability and enhance its operational reliability. This comprehensive approach will ensure that the proposed method remains effective and relevant across various operational environments. Moreover, integrating artificial intelligence and machine learning techniques presents opportunities for future enhancement, particularly in image-based distress detection and the automation of PCI calculation, supporting data-driven decision-making in pavement management. Future work will also explore the use of big data and deep learning techniques to identify the most promising approaches for developing case studies in airport environments.

CRediT authorship contribution statement

Ianca Feitosa: Writing – review & editing, Writing – original draft, Validation, Methodology, Investigation, Formal analysis, Conceptualization. **Jorge Gama:** Writing – review & editing, Methodology, Conceptualization. **Bertha Santos:** Writing – review & editing, Validation, Supervision, Investigation, Conceptualization. **Pedro G. Almeida:** Writing – review & editing, Validation, Supervision.

Declaration of Competing Interest

The authors declare the following financial interests/personal relationships which may be considered as potential competing interests: All authors report financial support was provided by Fundação para a Ciência e a Tecnologia (FCT). All authors declare that they have no known competing financial interests or personal relationships that could have appeared to influence the work reported in this paper.

Acknowledgments

The authors acknowledge the University of Beira Interior and GeoBioTec Research Unit through the strategic projects UIDB/04035/2020 (https://doi.org/10.54499/UIDB/04035/2020) and UIDP/04035/2020 (https://doi.org/10.54499/UIDP/04035/2020), funded by Fundação para a Ciência e a Tecnologia, IP/MCTES through national funds (PIDDAC), and CERIS—Civil Engineering Research and Innovation for Sustainability (ECI/04625/2020) for their support in conducting this study.

Data availability

Data will be made available on request.

References

[1] I. Feitosa, B. Santos, P.G. Almeida, Pavement inspection in transport infrastructures using unmanned aerial vehicles (UAVs), Art. no. 2207, Sustainability 16 (5) (Mar 6, 2024), https://doi.org/10.3390/su16052207.

[2] International Air Transport Association (IATA), "Aviation Ground Handling Report," Oct 24, 2018. [Online]. Available: ⟨https://www.iata.org/en/training/pages/aviation-ground-handling-report/⟩. Accessed: Jan. 19, 2024.

[3] International Air Transport Association (IATA), "Air Travel Growth Continues in March," May 4, 2023. [Online]. Available: https://www.iata.org/en/pressroom/2023-releases/2023-05-04-01/. Accessed: Oct. 15, 2024.

[4] S. Roh, J. Lee, I.J. Urbino, W. Lin, Y. Cho, "Airport pavement maintenance decision-making system with condition cases optimization,", Art. no. 13167, Appl. Sci. (Switz.) 13 (24) (2023), https://doi.org/10.3390/app132413167. Art. no. 13167.

[5] N.M. Kareem, A.T. Ibraheem, "Developing a frame design for airport pavements maintenance management system,", Int. J. Intell. Syst. Appl. Eng. 11 (4s) (2023) 498–508.

[6] B. Santos, P.G. Almeida, I. Feitosa, "Validation of an indirect data collection method to assess airport pavement condition,", Art. no. e00419, Case Stud. Constr. Mater. 13 (2020), https://doi.org/10.1016/j.cscm.2020.e00419.

[7] M.Y. Shahin. Pavement Management for Airports, Roads, and Parking Lots, 2nd ed., Springer, New York, NY, USA, 2005 https://doi.org/10.1007/b101538.

[8] A.P. Álvarez, J. Odieres-Meré, A.P. Loreiro, L. Marcos, "Opportunities in airport pavement management: integration of BIM, the IoT and DLT,", J. Air Transp. Manag. 7 (2020), https://doi.org/10.1016/j.jairtraman.2020.101941.

[9] A. Shtayat, S. Moridpour, B. Best, A. Shroff, D. Raol, "A review of monitoring systems of pavement condition in paved and unpaved roads,", J. Traffic Transp. Eng. 7 (5) (2020) 629–638, https://doi.org/10.1016/j.jtte.2020.03.004.

[10] Transportation Research Board (TRB), *Common Airport Pavement Maintenance Practices: A Synthesis of Airport Practice*, Airport Cooperative Research Program Synthesis 22, National Academy of Sciences, Washington, D.C., 2011.

[11] A. Di Graziano, A. Costa, E. Ragusa, "Using an airport pavement management system to optimize the influence of maintenance alternatives on operating conditions,", Art. no. 7158, Appl. Sci. (Switz.) 14 (16) (2024), https://doi.org/10.3390/app14167158. Art. no. 7158.

[12] I. Feitosa, *Validation of an indirect auscultation method for assessing the quality of airport pavements*, Master's dissertation, Civil Engineering - Geotechnics and Environment, Department of Civil Engineering and Architecture, University of Beira Interior (DECA-UBI), 2020. [Online]. Available: http://hdl.handle.net/10400.6/10620. Accessed: Feb. 23, 2024. [In Portuguese].

[13] I. Feitosa, B. Santos, and P.G. Almeida, "Validation of an indirect data collection method to assess airport pavement condition," in *Proceedings of the International Congress of Engineering – Engineering for Evolution (ICEUBI2019)*, Covilhã, Portugal, pp. 27–29, 2019. [In Portuguese].

[14] Federal Aviation Administration (FAA), *Guidelines and Procedures for Maintenance of Airport Pavements*, AC 150/5380–6 C, 2014. [Online]. Available: ⟨https://www.faa.gov/airports/resources/advisory_circulars/index.cfm/go/document.current/documentnumber/150_5380-6⟩. Accessed: Apr. 19, 2024.

[15] D. Lima, B. Santos, and P.G. Almeida, "Methodology to assess airport pavement condition using GPS, laser, video image and GIS," in *Pavement and Asset Management – Proceedings of the World Conference Pavement Asset Management (WCPAM 2017)*, Baveno, Italy, pp. 301–307, 2019.

[16] M.T. Miah, E. Oh, G. Chai, P. Bell, "An overview of the airport pavement management systems (APMS),", Int. J. Pavement Res. Technol. 13 (2020) 581–590, https://doi.org/10.1007/s42947-020-6011-8.

[17] Superintendency of Airport Infrastructure (SIA), *Airport Pavement Management System Manual - SGPA*, 1st ed., Feb. 2019. [In Portuguese].

[18] Federal Aviation Administration (FAA), *Airport Pavement Management Program (PMP)*, AC 150/5380-7B, 2014. [Online]. Available: ⟨https://www.faa.gov/documentLibrary/media/Advisory_Circular/150-5380-7B.pdf⟩. Accessed: Apr. 24, 2024.

[19] Applied Pavement Technology, Inc., *Washington Airport Pavement Management Manual*, prepared for the WSDOT Aviation Division and FAA Northwest Mountain Region, 2019. [Online]. Available: ⟨https://idea.appliedpavement.com/hosting/washington/reports/2018_WA_APMS_PM_Manual.pdf⟩. Accessed: Jul. 18, 2024.

[20] S. Saliminejad, N.G. Gharaibeh, "Impact of error in pavement condition data on the output of network-level pavement management systems, Transp. Res. Rec. (2013) 110–119, https://doi.org/10.3141/2366-13.

[21] A. Di Graziano, E. Ragusa, V. Marchetta, A. Palumbo, "Analyses of airport pavement management system during the implementation phase,", KSCE J. Civ. Eng. 25 (2021) 1424–1432, https://doi.org/10.1007/s12205-021-1884-x.

[22] L.M. Pierce, G. McGovern, and K.A. Zimmerman, *Practical Guide for Quality Management of Pavement Condition Data Collection,* Applied Pavement Technology, Inc., prepared for the Federal Highway Administration (FHWA), Washington, D.C., USA, Feb. 2013, 170 pp.

[23] E. Mansour, H. Dhasmana, and M. Hassan, "Using Advanced Modeling Techniques for Improving the Existing Airfield Pavement Management System Considering Structural and Functional Condition Indices," in *International Conference on Transportation and Development 2024: Pavements and Infrastructure Systems - Selected Papers*, pp. 45–58, 2024. doi: https://doi.org/10.1061/9780784485538.00.

[24] D. Lima, B. Santos, and P.G. Almeida, "Proposal of an Airport Pavement Maintenance Management System for Cape Verde," in *STARTCON19 - Int. Doctoral. Students Conf. + Lab Work. Civil Engineering*, KnE Engineering, pp. 49–60, 2020. doi: https://doi.org/10.18502/keg.v5i5.6917.

[25] L.A. Silva, H.S. Blas, D.P. García, A.S. Mendes, G.V. González, "An architectural multi-agent system for a pavement monitoring system with pothole recognition in UAV images,", Art. no. 21, Sensors 20 (2020) 6205, https://doi.org/10.3390/s20216205.

[26] M.J. Chin, P. Babashamsi, and N.I.M. Yusoff, "A comparative study of monitoring methods in sustainable pavement management system," *IOP Conf. Ser.: Materials Science and Engineering*, vol. 512, Art. no. 012039, 2019. doi: https://doi.org/10.1088/1757-899X/512/1/012039.

[27] K. Keegan and K. Jung, "Innovative approach to airfield pavement inspections and distress identification at Oakland International Airport," in *Proc. 9th International Conference on Managing Pavement Assets (ICMPA9)*, 2015. [Online]. Available: ⟨https://vtechworks.lib.vt.edu/bitstream/handle/10919/56397/ICMPA9-000070.PDF?sequence= 2&isAllowed=y⟩. Accessed: Aug. 10, 2024.

[28] E. Romero-Chambi, S. Villarroel-Quezada, E. Atencio, F. Muñoz-La Rivera, "Analysis of optimal flight parameters of unmanned aerial vehicles (UAVs) for detecting potholes in pavements,", Art. no. 4157, Appl. Sci. 10 (2020), https://doi.org/10.3390/app10124157. Art. no. 4157.

[29] Y. Tan, Y. Li, "UAV photogrammetry-based 3D road distress detection,", Art. no. 409, ISPRS Int. J. Geo-Inf. 8 (2019), https://doi.org/10.3390/ijgi8090409. Art. no. 409.

[30] N. Nappo, O. Mavrouli, F. Nex, C. Westen, R. Gambillara, A. Michetti, "Use of UAV-based photogrammetry products for semi-automatic detection and classification of asphalt road damage in landslide-affected areas,", Art. no. 106363, Eng. Geol. 294 (2021), https://doi.org/10.1016/j.enggeo.2021.106363. Art. no. 106363.

[31] L. Inzerillo, F. Acuto, G. Di Mino, M. Uddin, "Super-resolution images methodology applied to UAV datasets to road pavement monitoring,", Art. no. 171, Drones 6 (2022), https://doi.org/10.3390/drones6070171. Art. no. 171.

[32] C. Sierra, S. Paul, A. Rahman, A. Kulkarni, "Development of a cognitive digital twin for pavement infrastructure health monitoring,", Art. no. 113, Infrastructures 7 (2022), https://doi.org/10.3390/infrastructures7090113. Art. no. 113.

[33] L. Silva, H. Blas, D. García, A. Mendes, G. González, "An architectural multi-agent system for a pavement monitoring system with pothole recognition in UAV images,", Art. no. 6205, Sensors 20 (21) (2020), https://doi.org/10.3390/s20216205.

[34] Y. Wang, Y. Huang, W. Huang, "Crack junction detection in pavement image using correlation structure analysis and iterative tensor voting,", IEEE Access 7 (2019) 138094–138109, https://doi.org/10.1109/ACCESS.2019.2942318.

[35] J. Maslan, L. Cicmanec, "A system for the automatic detection and evaluation of the runway surface cracks obtained by unmanned aerial vehicle imagery using deep convolutional neural networks,", Art. no. 6000, Appl. Sci. 13 (10) (2023), https://doi.org/10.3390/app13106000.

[36] P. Alonso, J.A.I. Gordoa, J.D. Ortega, S. García, F.J. Iriarte, and M. Nieto, "Automatic UAV-based airport pavement inspection using mixed real and virtual scenarios," in *Proc. SPIE 12701, Fifteenth International Conference on Machine Vision (ICMV 2022)*, 2023, Art. no. 1270118, doi: https://doi.org/10.1117/12.2679734.

[37] M.A. Sourav, H. Ceylan, S. Kim, and M. Brynick, "Integration of small unmanned aircraft systems and deep learning for efficient airfield pavement crack detection and assessment," in *Proc. ASCE International Conference on Transportation and Development 2024: Transportation Safety and Emerging Technologies (ICTD 2024)*, 2024, doi: https://doi.org/10.1061/9780784485514.078.
[38] J. Wu, Y. Zhang, and X. Zhao, "Multi-task learning for pavement disease segmentation using wavelet transform," in *Proceedings of the 2022 International Joint Conference on Neural Networks (IJCNN)*, Padua, Italy, 2022, pp. 1–8, doi: https://doi.org/10.1109/IJCNN55064.2022.9892907.
[39] Z. Li, K. Zhao, and P. Zheng, "Research on Airport Pavement Condition Information System," in *Proceedings of the 2022 7th International Conference on Intelligent Computing and Signal Processing (ICSP)*, Xi'an, China, 2022, pp. 1400–1403, doi: https://doi.org/10.1109/ICSP54964.2022.9778714.
[40] D. Lima, *Airport Pavement Management System for Cape Verde, Master's dissertation*, Civil Engineering - Geotechnics and Environment, Department of Civil Engineering and Architecture, University of Beira Interior (DECA-UBI), 2016. [Online]. Available: ⟨http://hdl.handle.net/10400.6/6335⟩. Accessed: Mar. 12, 2024. [In Portuguese].
[41] L. Manganinho, *Development of a Pathology Database for Assessing Road Pavement Quality Using GPS, Video Image, and GIS*, Master's dissertation, Civil Engineering - Geotechnics and Environment, Department of Civil Engineering and Architecture, University of Beira Interior (DECA-UBI), 2013. [Online]. Available: ⟨http://hdl.handle.net/10400.6/3483⟩. Accessed: Mar. 13, 2024. [In Portuguese].
[42] A. Nogueira, *Assessment of Road Pavement Rutting Using Laser Scanning*, Master's dissertation, Civil Engineering - Geotechnics and Environment, Department of Civil Engineering and Architecture, University of Beira Interior (DECA-UBI), 2015. [Online]. Available: ⟨http://hdl.handle.net/10400.6/5132⟩. Accessed: Mar. 13, 2024. [In Portuguese].
[43] W. Eusébio, *Evaluation of Road Pavement Quality Using New Inspection Methods*, Master's dissertation, Civil Engineering - Geotechnics and Environment, Department of Civil Engineering and Architecture, University of Beira Interior (DECA-UBI), 2025. [Unpublished manuscript]. Provided by the author.
[44] B. Santos, P.G. Almeida, and L. Manganinho, "Data collection methodology to assess road pavement condition using GNSS, video image, and GIS," *IOP Conf. Ser.: Mater. Sci. Eng.*, vol. 603, Art. no. 042083, 2019. doi: http://doi.org/10.1088/1757-899X/603/4/042083.
[45] K. Sarkar, A. Shiuly, K.G. Dhal, "Revolutionizing concrete analysis: An in-depth survey of AI-powered insights with image-centric approaches on comprehensive quality control, advanced crack detection and concrete property exploration,", Constr. Build. Mater. 411 (2024) 134212, https://doi.org/10.1016/j.conbuildmat.2023.134212.
[46] R. Peck, T. Short, C. Olsen. Introduction to Statistics and Data Analysis, 6th ed., AP Edition, Cengage Learning, Boston, MA, USA, 2020.
[47] C. Weihs, K. Ickstadt, "Data Science: the impact of statistics,", Int. J. Data Sci. Anal. 6 (3) (2018) 189–194, https://doi.org/10.1007/s41060-018-0102-5.
[48] J. Maròco. Statistical Analysis with SPSS Statistics, 6th ed., Ediçôes Sílabo, Lda, Lisbon, Portugal, 2014.
[49] American Society for Testing and Materials (ASTM), *D5340-12, Standard Test Method for Airport Pavement Condition Index Surveys*, pp. 1–54, 2012. doi: https://doi.org/10.1520/D5340-12.2.
[50] M.F. Triola, Introduction to Statistics: Technology Update, LTC - Livros Técnicos e Científicos Editora Ltda, Rio de Janeiro, Brazil, 2013.
[51] E. Brunner, S. Domhof, F. Langer, Nonparametric Analysis of Longitudinal Data in Factorial Experiments, J. Wiley, New York, NY, 2002.
[52] K. Noguchi, Y.R. Gel, E. Brunner, F. Konietschke, "nparLD: an R software package for the nonparametric analysis of longitudinal data in factorial experiments,", J. Stat. Softw. 50 (12) (2012) 1–23, https://doi.org/10.18637/jss.v050.i12.
[53] Dubé M.O. Dubé, F. Desmeules, J. Lewis, R. Chester, J.S. Roy, "Will my shoulder pain get better? – secondary analysis of data from a multi-arm randomized controlled trial,", Physiotherapy 124 (2024) 65–74, https://doi.org/10.1016/j.physio.2024.01.003.
[54] J. Kloke, J.W. McKean. Nonparametric Statistical Methods Using R, 2nd ed., CRC Press, Boca Raton, FL, 2024 https://doi.org/10.1201/9781003039617.
[55] G.E.P. Box, G.M. Jenkins, G.C. Reinsel, G.M. Ljung. Time Series Analysis: Forecasting and Control, 5th ed., Wiley, Hoboken, NJ, 2015 https://doi.org/10.1111/jtsa.12194.
[56] G.M. Fitzmaurice, N.M. Laird, J.H. Ware, Applied Longitudinal. Analysis, 2nd ed., Wiley, Hoboken, NJ, 2011 https://doi.org/10.1002/9781119513469.
[57] B.T. West, K.B. Welch, A.T. Galecki. Linear Mixed Models: A Practical Guide Using Statistical Software, 3rd ed., Chapman and Hall/CRC, New York, 2022 https://doi.org/10.1201/9781003181064.
[58] US Army Corps of Engineers, *Asphalt Surfaced Airfield Paver Distress Identification Manual*, Champaign, IL: Construction Engineering Research Laboratory, 2009. [Online]. Available: ⟨https://www.faa.gov/documentLibrary/media/Advisory_Circular/Asphalt-Surfaced-Airfields-Distress-Manual.pdf⟩. Accessed: Aug. 25, 2024.
[59] IBM Corp., *IBM SPSS Statistics for Windows*, Version 27.0, Armonk, NY, 2020.
[60] R Core Team, *R: A Language and Environment for Statistical Computing*, Version 4.0.2, Vienna, Austria, 2020. [Online]. Available: https://www.r-project.org/. Accessed: Nov. 20, 2022.